

## NUCLEATION AND GROWTH OF CAVITIES AT DEFINED GRAIN BOUNDARIES IN BCC AND FCC BICRYSTALS

R.LOMBARD, H.VEHOFF\*

Cavity nucleation and cavity growth were measured and described quantitatively for a bcc and a fcc lattice. The creep tests were done on bicrystals (commercial iron silicon and an austenitic steel, X8 CrNiNb 1613 as models for bcc- and for fcc-lattices respectively). Cavity distribution functions of defined boundaries were measured as a function of the applied stress and the creep time. The results yielded the cavity nucleation and growth laws as well as the influence of external environments, free surfaces and particles on cavity nucleation for both crystal structures.

INTRODUCTION

Under creep or creep-fatigue loading, the nucleation and growth of cavities often controls the life of a polycrystalline component. These cavities preferentially nucleate at local stress concentrators like interfaces, particles or triple junctions (1). In polycrystals, their growth can be constrained by adjacent grains and depends critically on the orientation of the grain boundaries relative to the applied stress (2). A thorough understanding of cavity nucleation and growth is necessary to obtain reliable long term life predictions (3,4). Especially the preferential nucleation of cavities near free surfaces in even benign environments must be understood, since the linkage of these cavities yield to early crack nucleation in creep fatigue. In bicrystals (unconstrained flow), the nucleation and growth of cavities depend only on the material, the kind and distribution of particles, the applied stress, and the temperature. Early cavity nucleation due to incompatibility stresses, dislocation pile ups at grain boundaries, and external environments can be directly observed after cleaving the bicrystal along the boundary and evaluating the cavity distribution as a function of the distance from the free surface. In addition, bicrystals facilitate the quantitative comparison between theory and experiment.

\* Max-Planck-Institut für Eisenforschung GmbH, Abteilung Physikalische Metallkunde, Düsseldorf, West Germany

Therefore creep tests were conducted on stainless steel bicrystals (fcc) and on FeSi bicrystals (bcc) with the boundary plane oriented perpendicular to the applied stress. The particle distribution on the boundary plane was controlled by alloying and appropriate heat treatments. The cavity size distribution function (5) was measured for these bicrystals and compared with existing models for unconstrained cavity nucleation and growth (6).

### EXPERIMENTAL

Materials: Commercial iron silicon with 0.15 weight percent manganese and 0.02 weight percent sulphur was used as a model material for a ferritic steel. Austenitic stainless steel bicrystals were grown from X8 CrNiNb 16 13 melts.

Bicrystal preparation and grain boundary orientation: All bicrystals were grown with the Bridgman technique. The FeSi bicrystals were grown with  $45^\circ$ - $\langle 100 \rangle$ -asymmetrical tilt boundaries. These boundaries grew easily and yielded strong barriers for dislocations, which facilitates the nucleation of cavities at particles. For the austenitic steel two boundary orientations were examined, one with a  $45^\circ$ - $\langle 100 \rangle$  asymmetrical, the other with a  $22.5^\circ$ - $\langle 100 \rangle$  symmetrical tilt grain boundary.

Testing: Tension tests were carried out in a creep velocity range between 0.05 nm/sec and 10 nm/sec at  $600^\circ\text{C}$ . Some experiments were done in high vacuum to avoid early cavity nucleation and crack formation by intergranular oxidation, especially in FeSi.

Metallography: Two methods were used to measure the density and the radius of the cavities at the grain boundary.

1. Metallographic sections parallel to the specimen side surface were examined by SEM after prescribed increments of creep strain. The distance between and the radius of the cavities were measured with a lower detection limit of 30 nm for the cavity radius. Several tests with the same specimen could be made which reduces scatter due to different specimens, but only line sections perpendicular to the boundary plane were obtained. The results were evaluated with conventional techniques of quantitative metallography (7).
2. FeSi bicrystals could be cleaved along the grain boundary if the cavity distribution was high enough; the complete cavity distribution was obtained and evaluated inside a SEM.

### RESULTS

After appropriate heat treatments cavities in FeSi and austenitic stainless steel bicrystals were found on the grain boundary in air as well as in vacuum at  $600^\circ\text{C}$  for elongation rates between 0.05 and 10 nm/sec. However, if the kind of particles on the grain boundary was changed both materials failed by general creep without cavity formation.

FeSi bicrystals: Bicrystals containing niobium carbides never failed by cavitation, whereas crystals containing sulfur or MnS particles cavitared heavily. In air, cavities nucleated preferentially directly at the surface but even in vacuum in a distance of 300  $\mu\text{m}$  from the surface, preferentially nucleation and growth was observed. Hence, in addition to environmental effect incompatibility stresses support cavity nucleation and growth. This is supported by the fact, that near existing cracks, the cavity density decreases linearly with the distance from the crack tip (8).

Evaluating the cavity distribution at a fixed distance from the surface as a function of time and stress yielded that the number of cavities increased with time, and that the maximum of the cavity distribution function shifted toward lower cavities radii with increasing creep time for a given stress. Two typical distributions are given in Figure 1, after different creep times at the same stress. A cavity distribution for a relative short time is shown in Figure 2. The maximum is shifted to a greater radius and therefore cavities below this maximum value could be observed. The integral  $\int N(R)dR$  evaluated over the complete boundary where  $N(R)$  is the measured cavity size distribution function is given in Figure 3 obtained from tests at similar stresses after different creep times. The results showed that the cavity density rises sharply within the first hours, after 200 hours further damage occurs mainly by cavity growth. Similar curves were obtained for the cavity density as a function of stress. For low stresses, the cavity density is strongly stress dependent whereas for higher stresses the number of cavities is nearly independent of stress. These results clearly demonstrate that if the nucleation stress is overcome during loading for most of the particles, failure can simply be described by cavity growth and linkage.

Austenitic stainless steel bicrystals: For the strain and temperature range tested, nearly spherical cavities were observed. The material could not be cleaved intercrystallinely even after prolonged creep and at temperatures of liquid nitrogen. Therefore, the cavity distribution could only be examined in metallographic sections. Figure 4 shows typical cavity distributions as a function of the cavity radius for two different creep times at the same stress obtained from the same specimen. The qualitative behavior is similar as in FeSi, the maximum of the cavity distribution shifts to smaller radii with increasing creep time and the maximum and the number of cavities increases slowly with time. The stress dependence, however, is weaker than in FeSi. No gradient in the cavity distribution was observed as a function of the distance from the free surface, in addition, no preferential crack nucleation as well as increased cavity densities near introduced cracks were observed. For the stress range observed so far, a possible stress dependence of the cavity density lies within the scatter of the data, but still the cavity density is strain dependent, Figure 4. For the evaluation of a possible nucleation stress, tests at lower stresses and for shorter times are under way.

### DISCUSSION

Possible mechanisms for cavity growth are dislocation climb, diffusion or a mixture of both mechanisms. Evaluation of the cavity distribution function as a function of the applied strain rate, stress and temperature should yield information of the dominating growth mechanism. If this mechanism is known for a given set of experimental conditions, the cavity nucleation mechanism can be concluded from the experimental results. Knowing the stress and temperature dependence for the cavity behavior, crack growth by the nucleation, growth and coalescence of cavities can be modelled and compared with the experiments. Assuming power laws for cavity nucleation and growth, the following general distribution function can be obtained if continuity is assumed for the number of cavities moving from size class  $R$  to size class  $R + dR$  (6):

$$N(R, t) = \frac{A_2}{A_1} \cdot R^\beta \cdot t^{\alpha+\gamma} \cdot \left( 1 - \frac{1-\alpha}{1+\beta} \cdot \frac{R^{\beta+1}}{A_1 \cdot t^{1-\alpha}} \right)^{\frac{\alpha+\gamma}{1-\alpha}} \quad (1)$$

where  $\alpha, \beta$  are the exponents of the time dependence and the radius dependence of the growth law respectively,  $\gamma$  is the time dependence of the nucleation law. For power law growth,  $dR/dt$  should be proportional to  $R$  whereas for diffusion the dominant  $R$  dependence is  $1/R^2$ . For continuous and time independent nucleation and growth, these laws yield distributions with increasing cavity densities with decreasing  $R$  for power law, or increasing cavity densities with increasing  $R$  for diffusional growth, respectively. This is in contradiction to our measurements which yield a shift in the maximum with increasing creep strain or time for both steels. Due to the weak stress dependence observed diffusional growth must be assumed, this yields for the shift of the maximum:

$$R^3 = \frac{6 A_1 t^{1-\alpha}}{2 + \alpha + 3\gamma} \quad (2)$$

Hence  $\alpha$  must be greater than 1 to obtain a negative shift of the maximum. Therefore the cavity growth law must be explicitly time dependent. Together with the results for cavity nucleation this yields the following picture for damage by cavitation in bicrystals:

When a critical population of particles is available on the boundary, the number of cavities rises sharply if the nucleation stress is reached; when stress or strain increases further the number of cavities only weakly increases with time according to a nucleation law  $J^* = A_2 \cdot t^\gamma$  with  $\gamma$  in the range of -0.9 to -0.7. Since nucleation is explicitly time dependent the growth law must depend on time as well. The fits yield a law of the type  $dR/dt = A_1 \cdot R^{-2} \cdot t^{-\alpha}$  with  $\alpha$  between 1 and 2. Hence with increasing time and radius the growth rate of cavities decreases strongly.

No clear picture of the stress dependence is obtained so far. All tests show, that above the nucleation stress, in the austenitic steel further nucleation and growth is only weakly stress dependent as assumed for diffusion controlled cavitation. For the ferritic steel, however, nucleation was found to be clearly environment and stress dependent. Near crack tips and near the free surface definite higher cavity densities were observed with falling densities away from the stress risers. The examination of the cavity distribution within the surface area are under way. First results show a shift to larger cavities and higher densities which points to a strong stress dependence. Therefore in the case of FeSi we observe cavity growth by diffusion as well as by creep and a stress dependent nucleation.

Further measurements of the stress and time dependence are in progress to reduce the scatter for  $\alpha$ ,  $\beta$ ,  $\gamma$  and to obtain values for  $A_1$ ,  $A_2$  in dependence of the applied stress. Especially, tests at low stresses and short times are under way to measure the nucleation stress and to examine the development of the cavity distribution within the first hours of testing. Most tests so far were done in the long time region, duration of the tests between 100 hours up to 1200 hours. This means more than 10% of the total life time was spent before the cavity distribution was examined. In these cases the cavity population was completely developed and the distribution changes only slowly by growth.

#### SYMBOLS USED

$N(R)$  = cavity distribution function ( $m^{-2}$ )

$J^*$  = cavity nucleation rate ( $m^{-2}sec^{-1}$ )

#### REFERENCES

- (1) R.Raj, Acta Met. 26, 995 (1978)
- (2) B.F.Dyson, Metal Sci. 10, 349-353 (1976)
- (3) M.R.Myers and R.Pilkington, Mater.Sci.Eng. 95, 81 (1987)
- (4) N.G.Needham and T.Gladman, Metal Sci. 14, 64 (1980)
- (5) H.Riedel, Z.Metallkunde 76, 669 (1985)
- (6) H.Riedel, Fracture at High Temperatures, MRE Serie, Springer Verlag, Berlin (1987)
- (7) R.Weibel, Stereological Methods, Vol. 1+2, Academic Press, London (1979)
- (8) R.Lombard, H.Vehoff, Scripta Met., 24, 581 (1990)

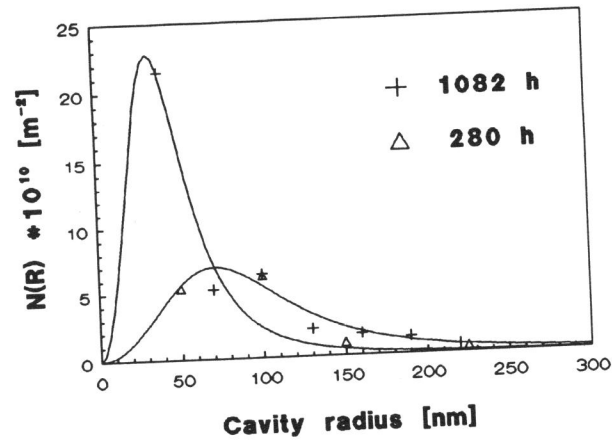


Figure 1. Cavity density as a function of the cavity radius in FeSi and the fitted cavity distribution functions for  $\sigma=24$  MPa and two creep times,  $t_1=280$  h,  $t_2=1082$  h

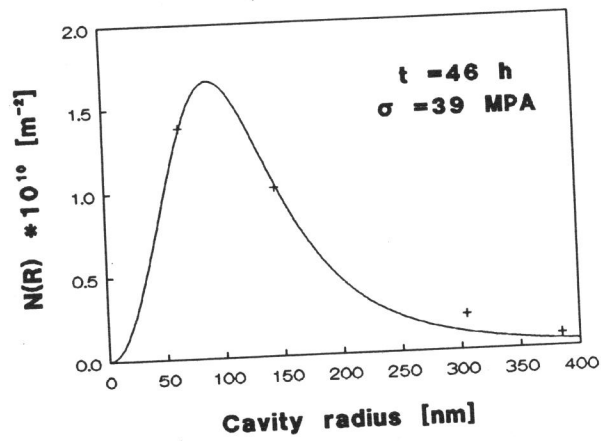


Figure 2. Cavity distribution in FeSi for  $t=46$  h and  $\sigma=39$  MPa

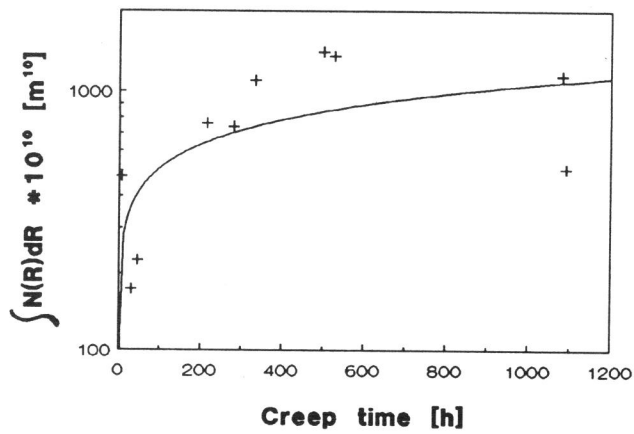


Figure 3.  $\int N(R)dR$  as a function of the creep time in FeSi

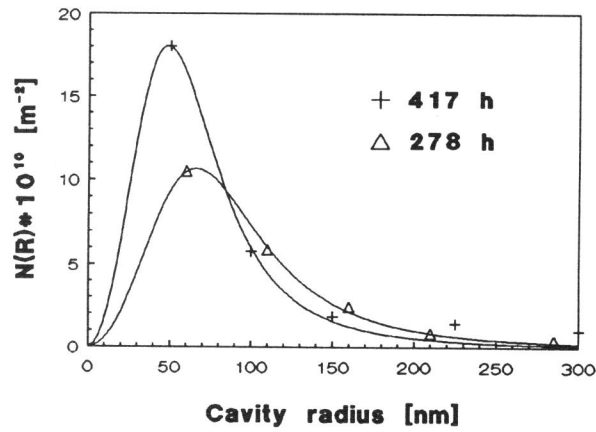


Figure 4. Cavity density as a function of the cavity radius in austenitic stainless steel and the fitted cavity distribution functions for  $\sigma=118$  MPa and two creep times,  $t_1=278$ h,  $t_2=417$ h obtained from the same specimen